



# Manganese octahedral molecular sieve (OMS-2) catalysts for selective aerobic oxidation of thiols to disulfides



Saminda Dharmarathna, Cecil K. King'onde, Lakshitha Pahalagedara, Chung-Hao Kuo, Yashan Zhang, Steven L. Suib\*

Department of Chemistry, University of Connecticut, 55 North Eagleville Road, U- 3060, Storrs, Connecticut 06269, United States

## ARTICLE INFO

### Article history:

Received 21 December 2012  
Received in revised form 26 July 2013  
Accepted 6 August 2013  
Available online 21 August 2013

### Keywords:

Self-assembly  
Catalysis  
Manganese oxide molecular sieve  
Nanorods  
Microstructure

## ABSTRACT

Selective aerobic oxidation of thiols to disulfides without any over oxidized products is studied using cryptomelane type manganese oxides (K-OMS-2) with a tunnel structure as catalysts. Using K-OMS-2 prepared by different synthetic procedures, complete conversion was obtained under air atmosphere without generating any overoxidized products. K-OMS-2 prepared by solvent free method (K-OMS-2<sub>SF</sub>) with the highest surface area ( $155 \pm 1 \text{ m}^2/\text{g}$ ) gave complete conversion, while materials prepared using hydrothermal method (K-OMS-2<sub>HY</sub>) with the lowest surface area ( $44 \pm 1 \text{ m}^2/\text{g}$ ) gave only 18% conversion at room temperature. Selective poisoning of the acid sites suggests that Lewis acid sites are the dominating active site during the reaction. Effects of surface area of the catalyst, solvent polarity, substrate effect, catalyst recyclability and temperature were studied. The catalyst could be recovered in the active form after the reaction without significant structural changes. The characterization of the catalyst using XRD, SEM, TGA, BET, TEM, and FT-IR are reported. The process developed is environmentally benign and is indeed heterogeneous.

© 2013 Elsevier B.V. All rights reserved.

## 1. Introduction

Oxidation of thiols to corresponding disulfides is an important class of reactions, due to the various important aspects of disulfide bonds, for instance in organic synthesis as an intermediate, [1–3] in biology as a structural feature which maintains the integrity of many biomolecules, [1,4–6] in vulcanization of rubber and elastomers, [7,8] and also in the petroleum industry [7–9] via removal of thiols by converting thiols to disulfides [9]. Oxidation of thiols to sulfur products that can be removed from petroleum products has become an important process. Thiols pose serious environmental, economical, and health concerns such as acid rain and poisoning of catalytic converters [10]. Many processes and catalysts have been developed for the removal of thiols from petroleum products.

The most commonly used process in petroleum industry is the Merox process [8,9,11]. However use of aqueous NaOH in the Merox process causes problems by generating caustic waste as a byproduct [9]. If not properly disposed, this caustic waste can be extremely harmful to the aquatic life. Many studies have been done to oxidize thiols however, these catalytic routes suffer from overoxidation [1–5,8]. High reactivity and weakness of S–S bonds cause overoxidation of disulfides to other products such as sulfinates, sulfoxides, sulfonates, and sulfonic acids [1,8,12]. Control of the product

selectivity or selective oxidation has attracted a great deal of interest due to many advantages of the process, such as minimal waste, less workup, short reaction time, and low cost and energy. Due to those attractive aspects of the selective oxidation process, an exponentially growing literature has developed over time. Many catalysts have been reported in the literature for the selective oxidation of thiols. Many of these catalysts are based on gold, [13] rhenium, [12] chromium, [7] lead, [10] cerium, [6] vanadium, [14] aluminum [15] halogen complexes, [16,17] Mn complexes, [18]  $\text{K}_3\text{PO}_4$ , [4] benzyltriphenylphosphonium peroxymonosulfate, [2] metal oxide frameworks, [1] Ni nanoparticles [5] Co–Fe composites, [8]  $\text{ZrO}_2$ , [9] and  $\text{NaI}/\text{H}_2\text{O}_2$  [3]. These catalytic routes require stoichiometric amounts of catalysts, expensive catalysts, high temperatures, long reaction times, generate undesirable toxic waste products, need complicated workup steps to remove the waste, and use complex catalysts which are homogeneous and therefore have recyclability problems when considering industrial practice. Some of these catalysts also require strong oxidizing agents such as peroxides and high partial pressures of oxygen which are hazardous reagents in transportation, storage, and handling [3,8,14]. Thus it is desirable to develop a heterogeneous catalytic process, which is highly selective, environmentally benign, less expensive, and consumes air as an oxidant.

Herein we developed a catalytic process for the oxidation of thiols using manganese oxide octahedral molecular sieve (OMS). These materials have high porosity and various different pore structures. Among them, cryptomelane (OMS-2) has gained a

\* Corresponding author. Tel.: +1 860 486 2797, fax: +1 860 486 2981.  
E-mail address: [steven.suib@uconn.edu](mailto:steven.suib@uconn.edu) (S.L. Suib).

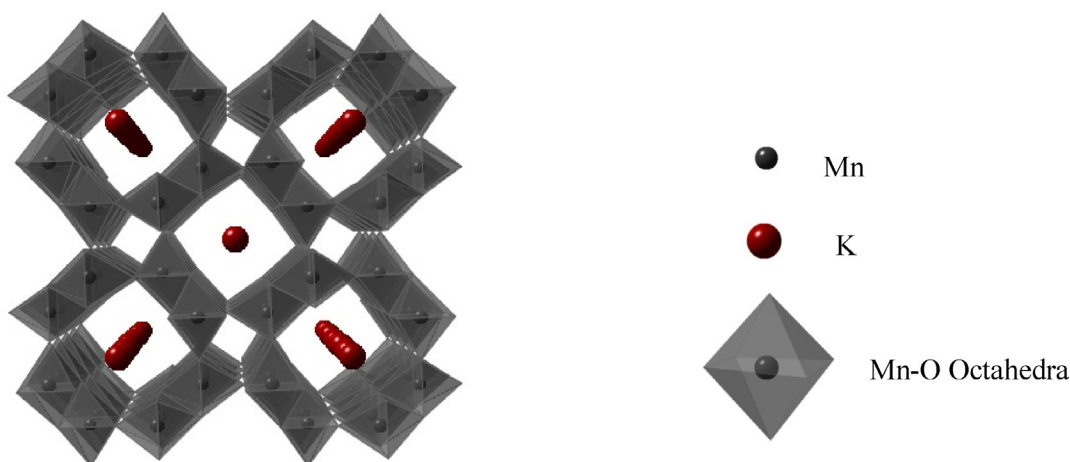


Fig. 1. Crystal structure of manganese oxide molecular sieves (OMS-2) created using crystal maker.

good reputation in redox catalysis. These materials have been synthesized in our laboratory and the characterizations are well documented [19–26]. The composition of cryptomelane (K-OMS-2) materials is  $\text{KMn}_8\text{O}_{16} \cdot n\text{H}_2\text{O}$  and they have tunnel-type structures consisting of  $2 \times 2$  edge shared  $\text{MnO}_6$  octahedra, [27,28] Fig. 1. The tunnels have dimensions of  $4.6 \text{ \AA} \times 4.6 \text{ \AA}$ . Potentiometric titrations have revealed average oxidation state of OMS-2 to be  $\sim 3.8$ , which is due to the presence of  $\text{Mn}^{2+}$ ,  $\text{Mn}^{3+}$ , and  $\text{Mn}^{4+}$  ions in the octahedral framework [25,27]. These materials have been used for many catalytic transformations such as styrene epoxidation, [29] cyclohexane oxidation, [30] oxidation of tetraline, [31] oxidation of 2,3,6-trimethylphenol (TMP), [32] oxidation of alcohol, oxidative coupling of benzyl amine, [33] decomposition of dye, [34] and also photo catalytic oxidation of 2-propanol [35].

The objective of this work was to develop an economical, environmentally benign, heterogeneous, and highly selective catalytic process utilizing K-OMS-2 as a catalyst, which is much cheaper than noble metal catalysts, and is less toxic than chromium, lead, or aluminum. In addition, air was used as an oxidant, which is greener than peroxides and more cost effective than using pure oxygen. Excellent conversion and selectivity toward disulfide was achieved even at room temperature and the process was also heterogeneous.

## 2. Experimental

### 2.1. Reagents

Thiophenol and all the other thiol substrates were purchased from Sigma–Aldrich. Potassium permanganate,  $\text{KMnO}_4$  and manganese(II) sulfate monohydrate,  $\text{MnSO}_4 \cdot \text{H}_2\text{O}$  were purchased from Sigma–Aldrich. Nitric acid 70% ( $\text{HNO}_3$ ) was purchased from Alfa Aesar. The solvents used in this work were purchased from commercial sources. All reagents were purchased from Aldrich and used as received, unless otherwise indicated.

### 2.2. Catalyst synthesis

K-OMS-2<sub>REF</sub> was prepared by conventional reflux methods reported in the literature [30]. A mixture of potassium permanganate solution (0.4 M, 225 mL), manganese sulfate hydrate solution (1.75 M, 67.5 mL) and, 6.8 mL of concentrated nitric acid was refluxed for 24 h. Preparation of K-OMS-2<sub>SF</sub> was carried out using a solvent free method as follows [19]: a mixture of potassium permanganate 9.84 g and manganese acetate tetrahydrate 22.05 g was ground until homogeneous in an agate mortar, the powder was then kept in a glass vial and heated up to  $80^\circ\text{C}$  for 4 h. A black

powder was obtained and was washed with deionized water and dried overnight at  $80^\circ\text{C}$ . A hydrothermal method [24] was employed for the synthesis of K-OMS-2 materials. Potassium sulfate, potassium persulfate, and manganese sulfate monohydrate in the molar ratio of 3:3:2 (totaling 32 mmol) were dissolved in 70 mL of DDW. The reaction mixture was then transferred into a 125 mL hydrothermal reactor vessel and kept in an oven at  $250^\circ\text{C}$  for 4 days. Microwave assisted synthetic route [21] was used to prepare K-OMS-<sub>MWREF</sub>. Potassium permanganate, 6.65 g was dissolved in 100 mL of DDW and was added dropwise to a solution containing 9.90 g of manganese sulfate monohydrate and 3.4 mL of concentrated nitric acid in 33 mL of DDW. Mixture was stirred for 15 min, and then 15 mL of dimethylsulfoxide solution was added to make 10% (V/V). The resulting brown slurry in a 250 mL three necked round bottom flask fitted with a reflux condenser and a fiber optic temperature probe was then placed in a CEM Mars 5 microwave accelerated reaction system. Microwave power was set to 300 W and temperature was set to  $100^\circ\text{C}$ . The reaction was carried out for 90 min. The materials synthesized using above mentioned methods were filtered and washed until the filtrate was neutral and at last dried overnight at  $120^\circ\text{C}$ .

### 2.3. Catalyst characterization

#### 2.3.1. Powder X-ray diffraction studies

X-ray diffraction studies were carried out for the samples prepared to confirm the structure and phase purity using a Rigaku Ultima IV diffractometer with  $\text{Cu K}\alpha$  radiation ( $\lambda = 0.15406 \text{ nm}$ ). A beam voltage of 40 kV and beam current of 44 mA in a continuous scan mode with a scanning rate of  $2.0^\circ \text{ s}^{-1}$  in the  $2\theta$  range from  $5^\circ$  to  $70^\circ$  was used. The phases were identified using The International Center for Diffraction Data (ICDD) database.

#### 2.3.2. Scanning electron microscopy

Morphologies of the materials were studied using Zeiss DSM 982 Gemini emission microscope equipped with a Schottky Emitter at an accelerating voltage of 2 kV having a beam current of  $1 \mu\text{A}$ . The samples were dispersed in ethanol and were then coated on a silicon wafer and kept under vacuum overnight to dry prior to analysis.

#### 2.3.3. Transmission electron microscopy

Micromorphology was studied by using transmission electron microscopy (TEM) and high resolution transmission electron microscopy (HR-TEM). TEM and HR-TEM studies were done with a JEOL 2010 UHR FasTEM operating at an accelerating voltage of

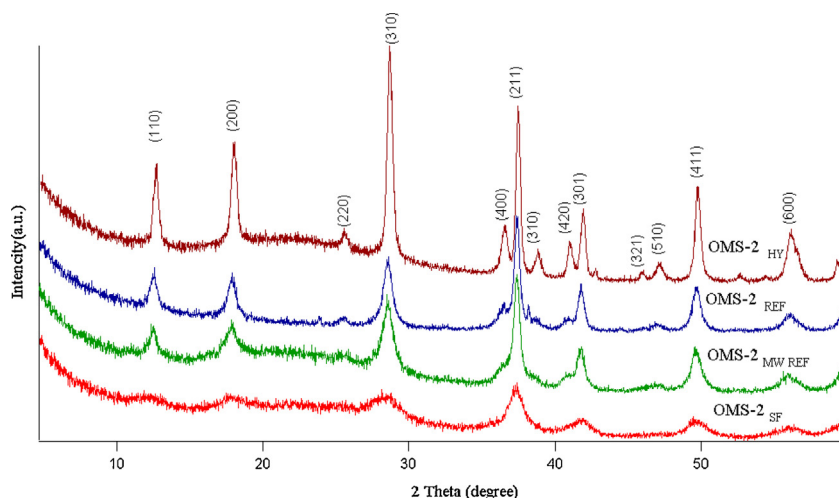


**Fig. 2.** XRD patterns of K-OMS-2 materials synthesized using different methods. Hydrothermal (OMS-2<sub>HY</sub>), reflux (OMS-2<sub>REF</sub>), microwave reflux (OMS-2<sub>MW REF</sub>), and solvent free (OMS-2<sub>SF</sub>).

200 kV and equipped with an energy dispersive X-ray analysis (EDS) system. The sample preparation was done by suspending the material in 2-propanol and then a drop of the suspension was placed onto a carbon-coated copper grid and allowed to dry.

#### 2.3.4. FT-IR and atomic absorption spectroscopy

Fourier transformation infra red (FT-IR) spectra were obtained, using a Thermo-Scientific Nicolet FT-IR Model 8700 (in the range 4000–400 cm<sup>-1</sup>) equipped with a DTGS detector. The dark brown manganese oxide powders were ground with dry KBr in a ratio of 1:100 and then pressed into self supporting pellets at about 10,000 psi. A leaching study was performed on the filtrate from the reaction and the analysis was done using a Perkin Elmer 3110 atomic absorption (AA) spectrometer.

#### 2.3.5. Thermal gravimetric analysis and N<sub>2</sub> sorption studies

Thermal stability studies of the materials were carried out by thermogravimetric analysis (TGA) using a Hi-Res TA instrument Model 2950. The temperature ramp for TGA was 20° min in nitrogen atmosphere. The nitrogen sorption experiments were carried out using a Quantachrome Autosorb iQ<sub>2</sub> surface area system. All samples were degassed at 150 °C for 12 h before the analysis. Determination of specific surface area was done using the Brunauer–Emmett–Teller (BET) method.

#### 2.4. Catalytic study

Reaction was carried out in a 50 mL three neck round bottom flask equipped with a reflux condenser, where one port served as a sampling port and the other was sealed during the course of the

reaction. In a typical reaction, thiol (2 mmol) was added to the solvent (10 mL) and the catalyst (50 mg) was added to a batch reactor open to air and the mixture was stirred using a magnetic stirrer. Aliquots were withdrawn from the reactor at time intervals and the identification of the reaction products and also the quantitative analyses were performed by GC-MS, using a HP 5971 mass selective detector coupled to a HP 5890 Series II gas chromatograph with a thermal conductivity detector (TCD) through an Agilent DB-17MS (17% polar cross-linked methyl siloxane) column with dimensions of 20 m × 0.18 mm × 0.18 μm.

In order to test the recyclability of the catalyst, the reaction mixture was centrifuged and catalyst was separated after the reaction. Then the spent catalyst was washed with acetone and then dried at 200 °C for 12 h. Then the regenerated catalyst was charged to a new reaction mixture as described above. The stability of the catalyst was tested by using the recovered catalyst in a new batch reaction without further treatment.

Selective poisoning of the Brønsted acid sites on the catalyst surface was done by using a literature reported method [44]. This was done by stirring K-OMS-2 in a 2 M NaOH solution for 1 h. The product, NaOH-OMS-2 was filtered, washed, and dried. The catalyst was then used in a batch reaction described above.

### 3. Results

#### 3.1. Morphology and phase evolution of K-OMS-2

X-Ray diffraction studies of K-OMS-2 synthesized using different synthetic techniques are shown in Fig. 2. All patterns agree with natural tetragonal cryptomelane with ICDD card number

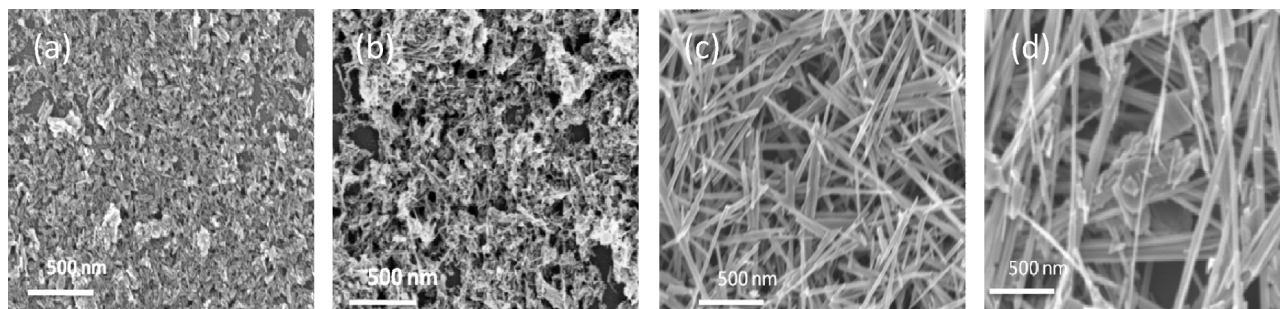


**Fig. 3.** FE-SEM images of different types of K-OMS-2. (a) K-OMS-2<sub>SF</sub>, (b) K-OMS-2<sub>MW</sub>, (c) K-OMS-2<sub>REF</sub>, (d) K-OMS-2<sub>HY</sub>.



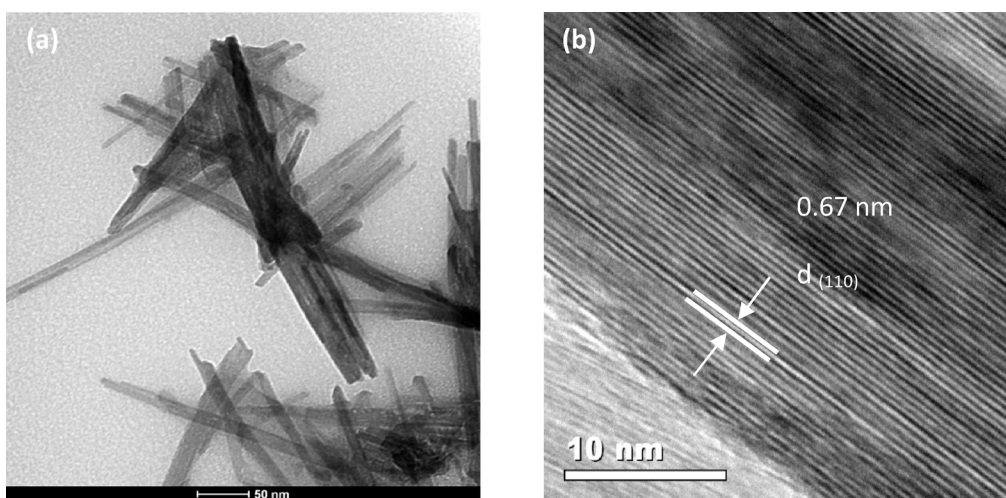


**Fig. 4.** TEM and HRTEM images of K-OMS-2<sub>REF</sub> materials. (a) Rod like morphology of K-OMS-2<sub>REF</sub> at low magnification (TEM). (b) Lattice fringes of (1 1 0) planes at high magnification (HRTEM).

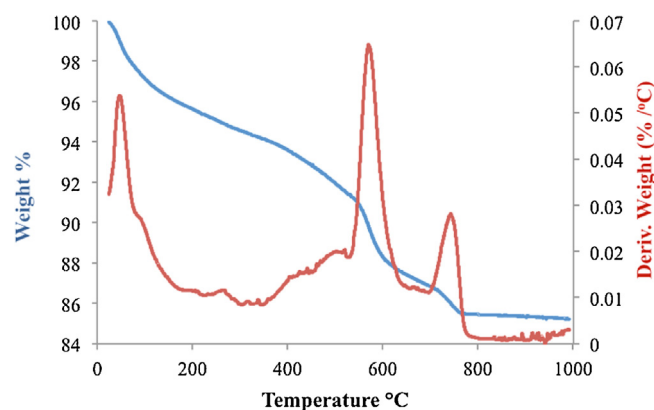
29-1020, having a chemical composition of  $\text{KMn}_8\text{O}_{16}$ . However the peak intensity drastically decreased from K-OMS-2<sub>HY</sub> to K-OMS-2<sub>SF</sub>. The peak broadening could also be seen in the K-OMS-2<sub>SF</sub> sample. FESEM was used to study the morphology of synthesized K-OMS-2 materials shown in Fig. 3. All the materials show needle like morphology, characteristic of OMS-2 materials. However, the particle sizes of the materials are significantly different. OMS-2 prepared by solvent free method has very short fiber lengths while OMS-2 synthesized by hydrothermal method had long fibers. Further microstructure characterization of K-OMS-2 materials was done using TEM. As shown in Fig. 4(a), all K-OMS-2 materials had a typical fiber like morphology, which is in agreement with FESEM results. HRTEM micrographs shown in Fig. 4(b) show lattice fringes of 0.67 nm, which can be indexed to the (1 1 0) planes as reported in the literature [26].

### 3.2. Structure, stability, and $\text{N}_2$ sorption studies

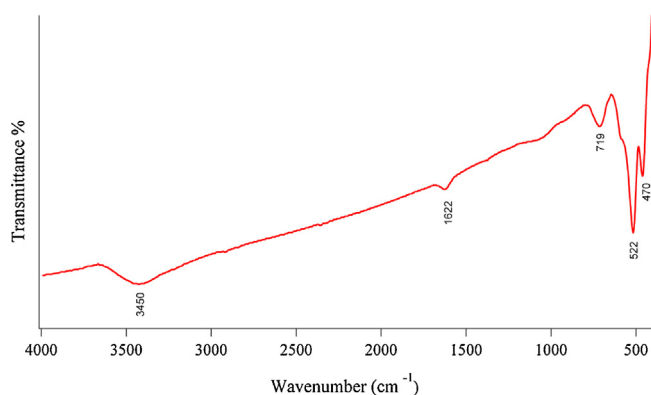
As synthesized K-OMS-2 materials were further characterized using FT-IR. Fig. 6 shows the typical IR spectra of K-OMS-2 materials. All materials show characteristic IR bands,  $\sim 400\text{--}800$ ,  $\sim 1619$ , and  $\sim 3413\text{ cm}^{-1}$  as reported in the literature [26,35,36]. Furthermore, thermal stability of K-OMS-2 was studied using TGA. Fig. 7 shows that three characteristic weight loss bands [19,21,37]  $\sim 50\text{--}100$ ,  $550\text{--}650$ , and  $700\text{--}800^\circ\text{C}$  were observed for all K-OMS-2 materials.  $\text{N}_2$  sorption studies for all synthesized K-OMS-2

materials show type II adsorption isotherms [21] which are shown in Figure S1 [38].

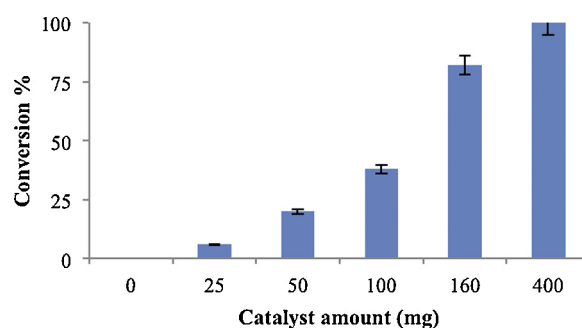
The catalyst was recovered after the reaction and the spent catalyst could be regenerated. Figure S2 in the supporting information section shows the XRD patterns of fresh and spent catalyst. No significant structural changes were observed. The regenerated catalyst was utilized in a separate reaction and the result is tabulated in Table 1, entry 1.1. The conversion for spent catalyst (35%) was nearly equal to the calculated conversion (37%) of the fresh catalyst. However, a significant loss of activity was seen when the catalyst was used without any regeneration during the recyclability test.



**Fig. 6.** Thermal gravimetric analysis of as synthesized K-OMS-2<sub>REF</sub> materials.



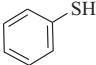
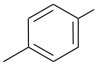
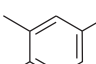
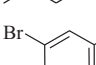
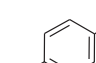
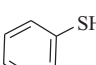
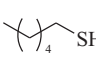
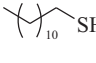
**Fig. 5.** Typical FTIR spectrum of K-OMS-2 materials.



**Fig. 7.** Effect of catalyst amount.

Reaction conditions: 2 mmol of thiophenol, 10 mL of acetonitrile as solvent, room temperature, and time 10 min.

**Table 1**  
Selective aerobic oxidation of thiols to disulfides using K-OMS-2.

Entry	Substrate	<sup>a</sup> Conv. (%)	<sup>b</sup> Sel. (%)
1		61	100
1.1	Recovered catalyst (30 mg)	35(37 <sup>c</sup> )	100
1.2	NaOH-OMS-2 (50 mg)	58	100
1.3	N <sub>2</sub> atmosphere	40	100
2		100	100
3		100	100
4		84	100
5		98	100
6		0	N/A
7		56	100
8		18	100

Reaction conditions: 50.0 mg of catalyst; 2 mmol of thiol;  $t = 30$  min and 10 ml of acetonitrile as solvent;  $T = 100^\circ\text{C}$ .

<sup>a</sup> Conversion (%) based on thiol

Conversion (%) based on substrate =  $[1 - ((\text{concentration of thiol after reaction}) \times (\text{concentration of thiol before reaction})^{-1})] \times 100$ .

<sup>b</sup> Selectivity based on disulfide, no other products were detected.

<sup>c</sup> Corresponding conversion with fresh catalyst.

After the first cycle 38 mg of catalyst was recovered, then the used catalyst was used in a second reaction without any treatment. The conversion was decreased to 22% as compared to 38 mg of fresh catalyst, where the conversion was calculated to be 46%. Then after the second reaction 27 mg of catalyst was recovered and used in a third reaction without any treatment. This gave a 10% conversion; similarly a substantial deactivation of the catalyst as compared to 27 mg of fresh catalyst was accompanied by a 33% conversion.

The determination of active sites involved in the reaction was studied by selectively poisoning one of the major active sites (Brønsted acid sites) on OMS-2. As synthesized K-OMS-2 was treated with NaOH in order to remove Brønsted acid sites selectively, and this NaOH-OMS-2 was used in a new reaction. According to the result is given in Table 1, entry 1.2 there was no significant change in conversion (58%) as compared to fresh K-OMS-2 (61%), which consists of both Lewis and Brønsted acid sites. Furthermore the role of air in the reaction was studied by using N<sub>2</sub> atmosphere in the reaction. The reaction vessel and reflux condenser was purged and sealed under N<sub>2</sub> and the reaction was carried out. The result is tabulated in Table 1, entry 1.3. The results show a decrease in conversion (40%) when N<sub>2</sub> was used, as compared to air (61%).

### 3.3. Effect of substrate

Aromatic and aliphatic thiol substrates, with different substituents attached, were studied for aerobic oxidation to corresponding disulfides. Table 1 summarizes the results which show that aromatic thiols, those with methyl groups (Table 1, entries



**Scheme 1.** Aerobic oxidation of thiols to disulfides.

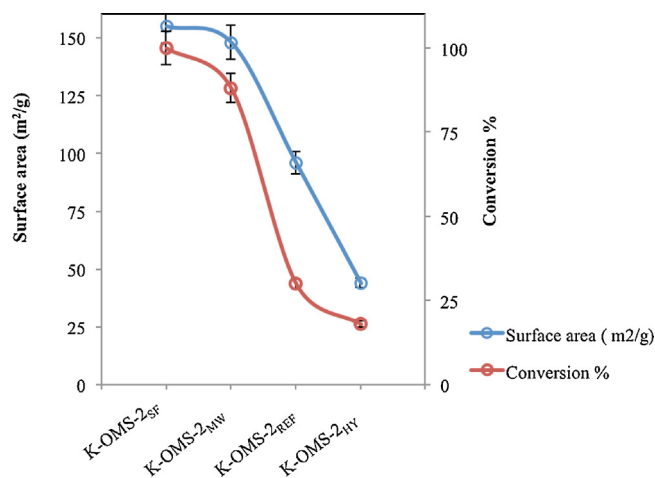


**Fig. 8.** Effect of surface area of catalyst on the reaction.

Reaction conditions: 50.0 mg of K-OMS-2<sub>R</sub> catalyst, 2 mmol of thiophenol, 10 mL of acetonitrile as solvent, room temperature, and time 1 h.

2 and 3) attached, gave complete conversion as compared to 61% conversion of thiophenol (Table 1, entry 1) where no additional groups are attached. On the other hand, when carboxylic acid groups are attached to the aromatic ring (Table 1 entry 6) no conversion was observed. Further substrates like 3-bromothiophenol and 4-chlorothiophenol gave 84% and 98% conversion respectively (Table 1, entries 4 and 5). For aliphatic thiols a lower conversion was obtained, as the carbon chain gets longer (Table 1, entries 7 and 8). Hexane thiol with C<sub>6</sub> chains gave 56% conversion while dodecane thiol with C<sub>12</sub> chain gave only 18% conversion. However, in both cases 100% selectivity was observed toward the corresponding disulfide. Further substrates such as thiophene and benzothiophene were used in which, the S atom was involved in an aromatic system did not yield corresponding disulfide or any other oxidation products as sulfoxide or sulfones.

### 3.4. Effect of catalyst amount

The effect of catalyst amount on the aerobic oxidation of thiophenol was studied. Catalyst amount was varied from 0 to 400 mg while keeping all other parameters the same. Fig. 7 shows that an increase of catalyst amount increases the conversion. When no catalyst was used, the reaction did not proceed. Even after 24 h no conversion was obtained.

### 3.5. Effect of catalyst surface area

The aerobic oxidation of thiol was carried out using K-OMS-2 catalyst synthesized using different synthetic techniques; solvent free (K-OMS-2<sub>SF</sub>, surface area 155 ± 1 m²/g), microwave reflux (K-OMS-2<sub>MWREF</sub>, surface area 148 ± 1 m²/g), conventional reflux (K-OMS-2<sub>REF</sub>, surface area 96 ± 1 m²/g) and, hydrothermal (K-OMS-2<sub>HY</sub>, surface area 44 ± 1 m²/g). The reaction was carried out in a batch reactor in an oil bath and the same conditions were used for all the reactions. The reaction was 100% selective toward the corresponding disulfide (Scheme 1). According to the results summarized in Fig. 8, catalysts prepared by solvent free method with the highest surface area gave the highest conversion (100%), while hydrothermally prepared catalysts with the lowest surface area

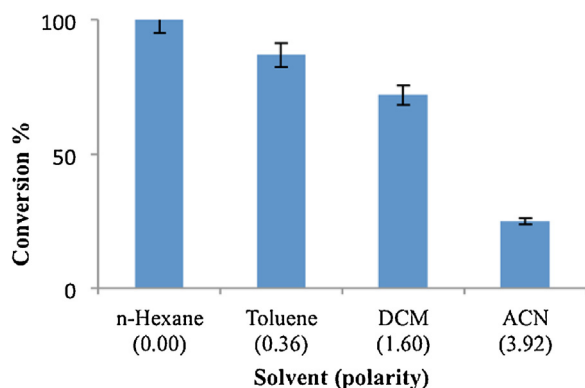


**Fig. 9.** Effect of solvent polarity on the reaction.

DCM: dichloromethane, ACN: acetonitrile

Reaction conditions: 50.0 mg of K-OMS-2<sub>R</sub> catalyst, 2 mmol of thiophenol, 10 mL of solvent, room temperature, and time 30 min.

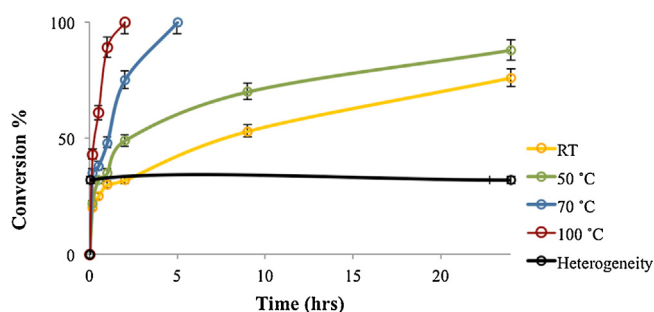


**Fig. 10.** Temperature and heterogeneity study for oxidation of thiol.

Reaction conditions: 50.0 mg of K-OMS-2<sub>R</sub> catalyst, 2 mmol of thiophenol, 10 mL of solvent.

yield the lowest conversion (18%). Selectivity was 100% for all the catalysts used.

### 3.6. Effect of solvent

The effect of solvents having different polarity was investigated on the aerobic oxidation of thiols as shown in Fig. 9. A non polar solvent n-hexane gives 100% conversion and acetonitrile which is a polar solvent gave only 32% conversion. Selectivity was 100% for all the different solvents.

### 3.7. Temperatures and heterogeneity of reaction

The effect of temperature on reaction was studied and results are shown in Fig. 10. Temperature of the reaction was varied from room temperature to 100 °C. Reaction was carried out for 24 h at room temperature and 50 °C in order to obtain 76% and 88% conversions respectively. When the temperature was increased to 70 °C and 100 °C complete conversion was obtained within 5 h and 2 h respectively. The kinetic study was carried out at 100 °C on thiophenol, aliquots from the reaction mixture were withdrawn and were analyzed using GC-MS. A plot of  $\ln$  [thiophenol] vs. time (s) showed a linear relationship, suggesting a first-order dependence on thiol as shown in Fig. 11. The heterogeneity of the reaction was tested by filtering off the catalyst after 30 min and allowing the reaction mixture to run for 24 h. The conversion did not change appreciably even after 24 h without catalyst. Catalyst leaching was tested by using AA spectroscopy and the results show 0.30 ppm of Mn and 0.90 ppm of K in the reaction filtrate after the reaction.

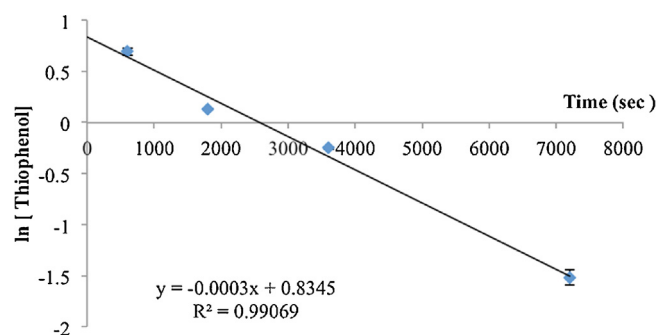


**Fig. 11.** Kinetic study for oxidation of thiol.

Reaction conditions: 50.0 mg of catalyst, 2 mmol of thiol, and 10 mL of acetonitrile as solvent;  $T = 100^\circ\text{C}$ .

## 4. Discussion

### 4.1. Structure and stability of K-OMS-2 catalysts.

Selective aerobic oxidation of thiols was carried out using manganese octahedral molecular sieve catalysts. Different synthetic techniques were used to control the particle size and surface area of the catalysts. Fig. 2 shows the XRD patterns of all the materials synthesized. K-OMS-2<sub>HY</sub> materials have narrow and intense XRD peaks as compared to K-OMS-2<sub>SF</sub> indicative of large crystallite sizes for K-OMS-2<sub>HY</sub> and smaller crystallite sizes for K-OMS-2<sub>SF</sub>. These results are in agreement with FESEM data shown in Fig. 3. The particle size increases in the order of K-OMS-2<sub>SF</sub>, K-OMS-2<sub>MWREF</sub>, K-OMS-2<sub>REF</sub>, and K-OMS-2<sub>HY</sub> materials. Fig. 4 shows a TEM micrograph with a typical fiber like morphology and HRTEM with well defined lattice fringes corresponding to (1 1 0) lattice planes of K-OMS-2<sub>REF</sub> materials as reported in the literature [26]. Further characterization of the catalysts was done using FTIR shown in Fig. 5. Typical FTIR spectra for K-OMS-2 materials as reported in the literature [21,36,39] were observed.

The MnO framework showed vibrational bands from 400 to 800  $\text{cm}^{-1}$  and the IR band at  $\sim 1619\text{ cm}^{-1}$  is due to water molecules in the tunnels. The band at  $\sim 3413\text{ cm}^{-1}$  is due to surface hydroxyl groups [36]. TGA analysis was done on the catalysts in order to study the thermal stability. Three major characteristic weight losses for OMS-2 materials were observed [21,39,38]. The first weight loss peak between 50 and 100 °C could be attributed to physisorbed water, and the weight loss at  $\sim 550\text{--}650^\circ\text{C}$  was due to the decomposition of manganese oxide to  $\text{Mn}_2\text{O}_3$ , and with further evolution of lattice oxygen this phase was reduced to  $\text{Mn}_3\text{O}_4$  giving rise to the weight loss  $\sim 700\text{--}800^\circ\text{C}$  [21,36,43].

### 4.2. Substrate effect

The K-OMS-2 catalyzed selective aerobic oxidation of different thiol substrates was studied (Table 1). Aromatic thiols having methyl groups showed a higher conversion (Table 1, entries 2 and 3) than thiophenol where no methyl groups are attached to benzene rings, (Table 1, entry 1). This could be due to the electron donating ability of the methyl groups. Aromatic thiols with carboxylic acid groups attached gave no conversion (Table 1, entry 6). Thiophenols with a halide (Br or Cl) attached gave 84% and 98% conversions respectively, which are lower than 100% when methyl groups are attached (Table 1, entries 2 and 3) and higher than 61% with thiophenol (Table 1, entry 1) where no group is attached. The reason for this observation could be due to both mild ring deactivation and the electron donating character of halides. Conversion for aliphatic thiols decreased when the carbon chain length increased. This may be due to the steric effects of the long carbon chain showing lower

conversion (Table 1, entries 5 and 6), a trend previously observed in the literature [1,14].

#### 4.3. Catalyst activity and solvent effect

According to the results summarized in Fig. 7, an increase in the amount of catalyst causes a consequent increase in the conversion. This could be due to a mass transfer effect; more catalyst could offer more reactive sites for the same amount of substrate. However the reaction did not proceed without catalyst, which means the reaction is indeed catalytic. Effect of surface area of the catalyst was also studied. When the surface area of the catalyst increased the conversion was also increased. This also could be due to mass transfer effects, since higher surface area could offer more active sites for the reaction to occur. From the FESEM images and BET surface area data, when the surface area of the catalyst increased the particle size also decreased. Therefore smaller particle size could also play a role in catalysis such as the ease of substrate molecules being able to diffuse to the active sites [40,41].

Hexane, toluene, dichloromethane, and acetonitrile were evaluated as solvents for the reaction and the non polar solvent n-hexane gave complete conversion, while acetonitrile with the highest polarity (3.92) among all the solvents studied gave the lowest conversion (32%). This could be because of competitive binding of high polar solvent molecules to the active sites of K-OMS-2 catalysts, which inhibits thiol binding. [42]

#### 4.4. Kinetics, heterogeneity, and recyclability

According to the results shown in Fig. 10, higher temperatures favor the oxidation of thiols and the rate of the reaction was higher at high temperatures. Investigation of heterogeneity and catalyst leaching during the reaction was done by filtering off the catalyst after 30 min and allowing the reaction mixture to continue for 24 h. Small amounts of Mn (0.30 ppm) and K (0.90 ppm) were found in the filtrate. However, there was no appreciable increase in the conversion when the catalyst was removed, Fig. 10. This suggests that the K-OMS-2 phase of the catalyst is important for the oxidation of thiols. The plot shown in Fig. 11 suggests a first order kinetics for oxidation of thiol. That is an indication of a rate-determining step involving a unimolecular intermediate. The possible unimolecular steps during the catalytic route would be the adsorption of thiol or the desorption of disulfide from the catalyst active site. However, more work is needed to distinguish the exact step. These adsorption and desorption could happen either due to Lewis or Brønsted acid sites. The results from the selective poisoning study did not show significant change with or without Brønsted acid sites on catalytic activity, suggesting that Lewis acid sites are the dominating active sites for the reaction. The mechanism could therefore involve adsorption of S atom on the Lewis acid site on the catalyst surface.

The typical mechanism for oxidation reactions on OMS-2 catalyst involves a Mars van Krevelen mechanism [20,39,43] in which, the adsorbed substrate molecules utilize the lattice oxygen from the OMS-2 structure and later these lattice oxygen get replenished by oxygen in the atmosphere. The results are tabulated in Table 1, entry 1.3 and show that, when air was eliminated the conversion decreased. This was a trend observed in our previous work [39] for oxidation reactions on OMS-2.

## 5. Conclusion

Herein we report a highly active, less expensive, and environmentally benign process for the aerobic oxidation of thiols under mild and alkaline free conditions. The process was 100% selective for disulfides. The reaction was truly catalytic and heterogeneous. By altering the solvent and catalyst amount, complete conversion

with 100% selectivity at ambient temperature was obtained. Catalyst could be recovered in the active form after the reaction without significant structural changes. The simplicity of the operation and no caustic waste byproduct generation are attractive aspects of this novel process and potentially could be used for large-scale industrial applications.

## Acknowledgments

Authors would like to thank the Chemical Sciences, Geosciences, and Biosciences Division, Office of the Basic Energy Sciences, Office of Science, and U.S. Department of Energy for support of this work under grant DE-FG02-86ER13622-A000.

## Appendix A. Supplementary data

Supplementary data associated with this article can be found, in the online version, at <http://dx.doi.org/10.1016/j.apcatb.2013.08.002>.

## References

- [1] A. Dhakshinamoorthy, M. Alvaro, H. Garcia, *Chemical Communications* 46 (2010) 6476–6478.
- [2] A.R. Hajipour, S.E. Mallakpour, H. Adibi, *Journal of Organic Chemistry* 67 (2002) 8666–8668.
- [3] M. Kirihaara, Y. Asai, S. Ogawa, T. Noguchi, A. Hatano, Y. Hirai, *Synthesis* (2007) 3286–3289.
- [4] A.V. Joshi, S. Bhusare, M. Baidossi, N. Qafisheh, Y. Sasson, *Tetrahedron Letters* 46 (2005) 3583–3585.
- [5] A. Saxena, A. Kumar, S. Mozumdar, *Journal of Molecular Catalysis A: Chemical* 269 (2007) 35–40.
- [6] C.C. Silveira, S.R. Mendes, *Tetrahedron Letters* 48 (2007) 7469–7471.
- [7] S. Ghammamy, M. Tajbakhsh, *Journal of Sulfur Chemistry* 26 (2005) 145–148.
- [8] L. Menini, M.C. Pereira, A.C. Ferreira, J.D. Fabris, E.V. Gusevskaya, *Applied Catalysis A: General* 392 (2011) 151–157.
- [9] D. Jiang, G. Pan, B. Zhao, G. Ran, Y. Xie, E. Min, *Applied Catalysis A: General* 201 (2000) 169–176.
- [10] J.P. Nehlsen, J.B. Benziger, I.G. Kevrekidis, *Energy and Fuels* 18 (2004) 721–726.
- [11] D. Xia, Y. Su, J. Qian, *Industrial and Engineering Chemistry Research* 34 (1995) 2001–2005.
- [12] J.B. Arterburn, M.C. Perry, S.L. Nelson, B.R. Dible, M.S. Holguin, *Journal of the American Chemical Society* 119 (1997) 9309–9310.
- [13] A. Corma, T. Rodenas, M.J. Sabater, *Chemical Science* (2012).
- [14] M. Kirihaara, K. Okubo, T. Uchiyama, Y. Kato, Y. Ochiai, S. Matsushita, A. Hatano, K. Kanamori, *Chemical and Pharmaceutical Bulletin* 52 (2004) 625–627.
- [15] A. Ghorbani-Choghamarani, M. Nikoorazm, H. Goudarziashar, B. Tahmasbi, *Bulletin of the Korean Chemical Society* 30 (2009) 1388–1390.
- [16] M.A. Zolfigol, G. Chehardoli, S. Salehzadeh, H. Adams, M.D. Ward, *Tetrahedron Letters* 48 (2007) 7969–7973.
- [17] N. Shefer, M. Carmeli, S. Rozen, *Tetrahedron Letters* 48 (2007) 8178–8181.
- [18] H. Golchoubian, F. Hosseini, Catalysis Communications 8 (2007) 697–700.
- [19] Y. Ding, X. Shen, S. Sithambaram, S. Gomez, R. Kumar, V.M.B. Crisostomo, S.L. Suib, M. Aindow, *Chemistry of Materials* 17 (2005) 5382–5389.
- [20] V.D. Makwana, S. Young-Chan, Amy R. Howell, Steven, L. Suib, *Journal of Catalysis* 210 (2002) 46–52.
- [21] E.K. Nyutu, C. Chen, S. Sithambaram, V.M.B. Crisostomo, S.L. Suib, *Journal of Physical Chemistry C* 112 (2008) 6786–6793.
- [22] A. Onda, S. Hara, K. Kajiyoshi, K. Yanagisawa, *Applied Catalysis A* 321 (2007) 71–78.
- [23] Y. Yin, W. Xu, R. DeGuzman, S.L. Suib, C.L. O'Young, *Inorganic Chemistry* 33 (1994) 4384–4389.
- [24] J. Yuan, K. Laubernds, J. Villegas, S. Gomez, S.L. Suib, *Advanced Materials* 16 (2004) 1729–1732.
- [25] J. Yuan, W. Li, S. Gomez, S.L. Suib, *Journal of the American Chemical Society* 127 (2005) 14184–14185.
- [26] C.K. King'ndu, N. Opembe, C. Chen, K. Ngala, H. Huang, A. Iyer, H.F. Garcés, S.L. Suib, *Advanced Functional Materials* 21 (2011) 312–323.
- [27] S.L. Suib, *Accounts of Chemical Research* 41 (2008) 479–487.
- [28] S.L. Suib, *Journal of Materials Chemistry* 18 (2008) 1623–1631.
- [29] R. Ghosh, X. Shen, J.C. Villegas, Y. Ding, K. Malinger, S.L. Suib, *Journal of Physical Chemistry B* 110 (2006) 7592–7599.
- [30] R. Kumar, S. Sithambaram, S.L. Suib, *Journal of Catalysis* 262 (2009) 304–313.
- [31] S. Sithambaram, E.K. Nyutu, S.L. Suib, *Applied Catalysis A* 348 (2008) 214–220.
- [32] N.N. Opembe, C.K. King'ndu, S.L. Suib, *Catalysis Letters* 142 (2010) 427–432.



- [33] S. Dharmarathna, S. Sithambaram, E.K. Nyutu, S.L. Suib, Abstract of Papers, CATL-024, in: 238th ACS National Meeting, Washington, DC, United States, August 16–20, 2009, 2009.
- [34] T. Sriskandakumar, N. Opembe, C. Chen, A. Morey, C. King'ondou, S.L. Suib, *Journal of Physical Chemistry A* 113 (2009) 1523–1530.
- [35] A. Iyer, H. Galindo, S. Sithambaram, C. King'ondou, C. Chen, S.L. Suib, *Applied Catalysis A* 375 (2010) 295–302.
- [36] G. Qiu, H. Huang, S. Dharmarathna, E. Benbow, L. Stafford, S.L. Suib, *Chemistry of Materials* 23 (2011) 3892.
- [37] K.A. Malinger, Y. Ding, S. Sithambaram, L. Espinal, S. Gomez, S.L. Suib, *Journal of Catalysis* 239 (2006) 290–298.
- [38] N.N. Opembe, C.K. King'ondou, A.E. Espinal, C. Chen, E.K. Nyutu, V.M. Crisostomo, S.L. Suib, *Journal of Physical Chemistry C* 114 (2010) 14417–14426.
- [39] S. Dharmarathna, C.K. King'ondou, W. Pedrick, L. Pahalagedara, S.L. Suib, *Chemistry of Materials* 24 (2012) 705–712.
- [40] G. Jia, H. Ma, Y. Tan, Y. Han, *Industrial and Engineering Chemistry Research* 44 (2005) 2011–2015.
- [41] V. Schwartz, D.R. Mullins, W. Yan, B. Chen, S. Dai, S.H. Overbury, *Journal of Physical Chemistry B* 108 (2004) 15782–15790.
- [42] S. Sithambaram, L. Xu, C. Chen, Y. Ding, R. Kumar, C. Calvert, S.L. Suib, *Catalysis Today* 140 (2009) 162–168.
- [43] H. Genuino, S. Dharmarathna, E. Njagi, Michael C. Mei, S.L. Suib, *Journal of Physical Chemistry C* 116 (2012) 12066–12078.
- [44] J. Luo, Q. Zhang, J. Martinez, S.L. Suib, *Journal of the American Chemical Society* 130 (2008) 3198–3232.